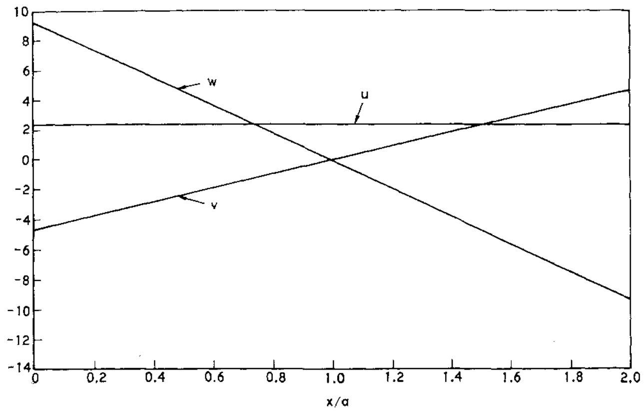

Fig. 1 Buckling mode for $EI_x/Dl = 90$ ($n = 2$).

simply supported edges are then given by $EI_x/Dl = 0$ and $EI_x/Dl = \infty$, respectively. Furthermore, because η is a large number, it may be seen from Eqs. (4) that α and β, which characterize the deviation of the equilibrium state from the membrane state, are small numbers relative to unity and, consequently, that their effect in Eq. (20) is practically negligible. Making this approximation, for the previously defined structure Eq. (20), reduces to, for $n = 2$,

$$\bar{P}/P_0 = 0.00735[1 + 3(EI_x/Dl)/2] \qquad (23)$$

In Table 2 are tabulated the upper bound values $\bar{P}/P_0$ along with the computer solution P^*/P_0 for $n = 2$, for which the equilibrium state was also taken to be the membrane state. It is observed that P^* follows $\bar{P}$ very closely up to about $EI_x/Dl = 90$, at which point $\bar{P}$ becomes greater than P_0. For $EI_x/Dl > 90$, P^* is given very accurately by P_0.

Figures 1 and 2 show the buckling modes obtained by the computer program for the cases $EI_x/Dl = 90$ and 100, respectively. In spite of the closeness of the buckling loads for these two cases, the buckling modes are seen to be of entirely different character. For $EI_x/Dl = 90$, the buckling mode is still highly inextensional and is given very accurately by Eqs. (5) with $B = 0$. Thus, as EI_x/Dl grows from 0 to 90, although P^* grows from less than 1% of P_0 to almost P_0, the buckling mode shapes have practically no change. It follows that, in this range, as EI_x/Dl increases, the increase in buckling load is caused essentially by the increase in flexural strain energy of the rings in their buckled state. On the other hand, for $EI_x/Dl = 100$, the buckling mode is no longer inextensional, and, in fact, approximates very closely the sinusoidal mode shape of the classical solution, i.e., for $EI_x/Dl = \infty$. Specifically, it is noted that Flugge's solution[7] for $t/r = 1.095 \times 10^{-2}$ and $\nu = \frac{1}{6}$ predicts a buckling mode with eleven axial half-waves for a shell of half-length $l/r = 1$.

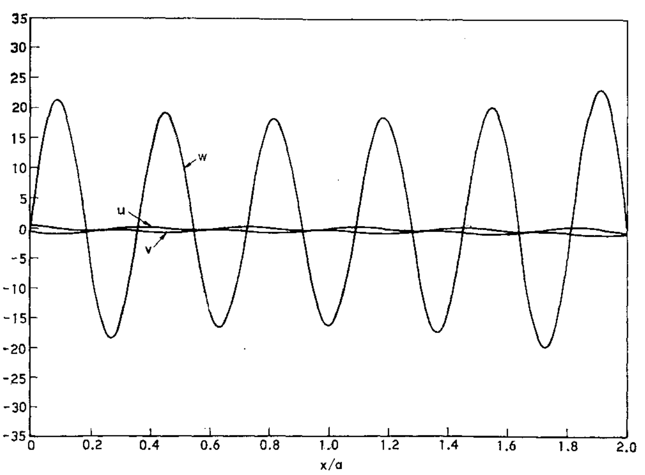

Fig. 2 Buckling mode for $EI_x/Dl = 100$ ($n = 2$).

Although t/r and ν considered here are slightly different, the buckling mode obtained for $EI_x/Dl = \infty$ has also eleven axial half-waves, as does the buckling mode for $EI_x/Dl = 100$ (cf. Fig. 2). Note also that whereas the inextensional mode of Fig. 1 has its maximum displacements at the rings, the mode of Fig. 2 has small, almost negligible, displacements at the rings. Since, in the latter case, the shell has high extensional strain energy in the buckling mode, the shell strain energy completely dominates the ring strain energy. This explains why further increases in ring rigidity have such a slight effect.

From the foregoing results, it may be expected that there exists a critical rigidity ratio $(EI_x/Dl)^*$, below which the ring strain energy controls the buckling and the mode is inextensional, and above which the ring strain energy is negligible and, to the degree of approximation used, the buckling mode is practically given by the classical solution for simply supported edges. By extrapolating the buckling load curves of these two different modes of buckling to their point of intersection, it is determined that $(EI_x/Dl)^* \approx 90.5$. For this value of the rigidity ratio, the buckling loads of the two modes coincide and there are two bifurcation paths emanating from the corresponding equilibrium state.

References

[1] Nachbar, W. and Hoff, N. J., "The buckling of a free edge of an axially-compressed circular cylindrical shell," Quart. Appl. Math. **20**, 267–277 (1962).

[2] Hoff, N. J. and Soong, T., "Buckling of circular cylindrical shells in axial compression," Dept. of Aeronautics and Astronautics, Stanford Univ., SUDAER 204 (August 1964).

[3] Almroth, B. O., "Influence of imperfections and edge restraint on the buckling of axially compressed cylinders," NASA CR-432 (April 1966).

[4] Novozhilov, V. V., *Foundations of the Nonlinear Theory of Elasticity* (Graylock Press, Rochester, New York, 1953), Article 45.

[5] Love, A. E. H., *The Mathematical Theory of Elasticity* (Dover Publications Inc., New York, 1944), Articles 319 and 321.

[6] Cohen, G. A., "Computer analysis of asymmetric free vibrations of ring-stiffened orthotropic shells of revolution," AIAA J. **3**, 2305–2312 (1965).

[7] Flugge, W., *Stresses in Shells* (Springer-Verlag, Berlin, 1962), p. 427.

A Simple Calibration Technique for Skin Friction Balances

J. W. Headley*
Northrop Norair, Hawthorne, Calif.

Skin friction balances of the floating element type (Ref. 1, for example) usually are designed to have full-scale deflection under very small loads, typically of the order 1×10^{-2} lb. The accurate calibration of such a balance, particularly in situ in a wind tunnel, demands a careful approach. One of the most common techniques is to attach a thread to the balance element, run this over a low friction pulley, and then to a weight pan. Calibration then consists of applying known weights and noting the balance output.

An alternate approach is suggested here which removes the need for a pulley system, and hence the unknown frictional load in the system. Three threads attached at a common point are connected, respectively, to the balance element, the weight pan, and a suitable rigid point, as shown in Fig. 1.

Received May 9, 1966; revision received June 2, 1966.

* Senior Engineer, Gas Dynamics Research. Member AIAA.

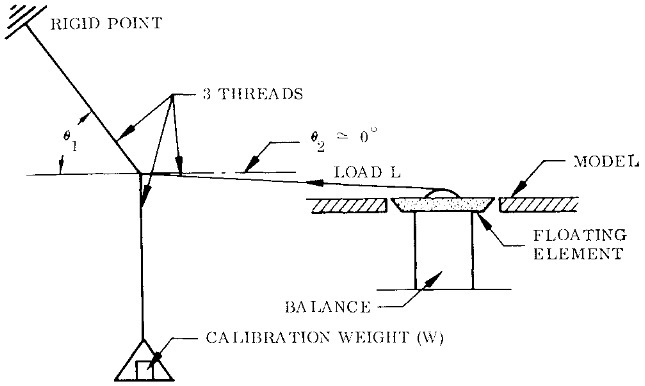

Fig. 1 Schematic of the calibration technique.

Any percent of the weight W can be applied to the balance by a suitable choice of the angle θ.

For the general case of $\theta_2 \neq 0°$, we have the calibration load $C = L\cos\theta_2 = W/\tan\theta_1 \pm \tan\theta_2$. Calibration error produced by θ_2 being small but not exactly equal to zero is given by $(dC/d\theta_2)\ \alpha(1/\tan^2\theta_1)$ and will be minimized by making θ_1 as large as is practical. The system is, of course, friction free.

Reference

[1] Dhawan, S., "Direct measurements of skin friction," NACA Rept. 1121 (1953).

Steady-State Response of Beams Supported on Nonlinear Springs

A. V. Srinivasan*
Kaman Aircraft Corporation, Bloomfield, Conn.

THIS technical note presents a study of the free and forced vibration response of beams resting on a hard spring of the Duffing type. The Fourier series method and the method due to Ritz are applied and comparison is made. It will be shown that the latter method is much simpler to apply to such problems.

The Fourier technique was used by Paslay and Gurtin[1] on the problem of a vibrating elastic system supported on a nonlinear spring. A brief discussion of the method is presented below to aid the comparison of the methods. The steady-state displacement of a linear undamped system to a force system whose components vary sinusoidally is expressible in the form[1]

$$w_i = \sum_j M_{ij}(\Omega_j)F_j \sin\Omega_j t \tag{1}$$

where

w_i = displacement at i
M_{ij} = influence function (i.e., displacement at i due to a force of unit amplitude at j, oscillating with circular frequency Ω_j)
F_j = amplitude of the external force at j
t = time

The force induced at 0 and the displacement w at 0 may be

Received February 28, 1966; revision received May 6, 1966.
* Research Specialist.

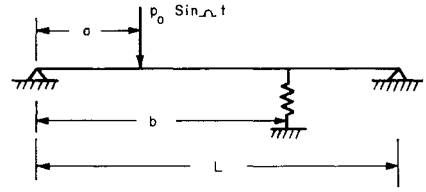

Fig. 1 Simply supported beam resting on a hard spring.

expanded as

$$F_0 \doteq F_{01}\sin\Omega t + F_{03}\sin 3\Omega t + \ldots \tag{2}$$

and

$$w_0 \doteq w_{01}\sin\Omega t + w_{03}\sin 3\Omega t + \ldots \tag{3}$$

Restricting the summation to two terms and with $F_0 = k(w_0 + \epsilon w_0^3)$ where k is spring constant and ϵ is the nonlinearity factor, it can be shown that

$$F_0 = \sin\Omega t\{kw_{01} + k\epsilon\tfrac{3}{4}w_{01}^3 + k\epsilon\tfrac{3}{2}w_{01}w_{03}^2 - \tfrac{3}{4}k\epsilon\, w_{01}^2w_{03}\} + \sin 3\Omega t\{kw_{03} - k\epsilon\tfrac{1}{4}w_{01}^3 + \tfrac{3}{4}k\epsilon\, w_{03}^3 + \tfrac{3}{2}k\epsilon\, w_{01}^2 w_{03}\} + \text{coefficients on } \sin 5\Omega t,\ \sin 7\Omega t, \text{ etc.} \tag{4}$$

Thus,

$$F_{01} = k\{w_{01} + \epsilon(\tfrac{3}{4}w_{01}^3 + \tfrac{3}{2}w_{01}\,w_{03}^2 - \tfrac{3}{4}w_{01}^2 w_{03})\} \tag{5}$$

and

$$F_{03} = k\{w_{03} + \epsilon(\tfrac{3}{4}w_{03}^3 + \tfrac{3}{2}w_{01}^2 w_{03} - \tfrac{1}{4}w_{01}^3)\} \tag{6}$$

But

$$w_0 = F_1 M_{01}(\Omega)\sin\Omega t + F_{01}M_{00}(\Omega)\sin\Omega t + F_{03}M_{00}(3\Omega)\sin 3\Omega t \tag{7}$$

Substituting for F_{01}, F_{03} from (5) and (6), and equating the coefficients on $\sin\Omega t$ and $\sin 3\Omega t$, w_{01} and w_{03} may be shown to be

$$w_{01} = F_1 M_{01}(\Omega) - kM_{00}(\Omega)\{w_{01} + \epsilon(\tfrac{3}{4}w_{01}^3 + \tfrac{3}{2}w_{01}\,w_{03}^3 - \tfrac{3}{4}\,w_{01}^2\,w_{03})\} \tag{8}$$

$$w_{03} = M_{00}(3\Omega)\,k\{w_{03} + \epsilon(\tfrac{3}{4}w_{03} + \tfrac{3}{2}\,w_{01}^2 w_{03} - \tfrac{1}{4}w_{01}^3)\} \tag{9}$$

Equations (8) and (9) provide the desired response equations at 0. The aforementioned technique first will be applied to the case of a simple beam resting on a nonlinear spring at some position along the span, as shown in Fig. 1.

Using standard methods available in Structural Dynamics it may be shown that

$$M_{ba}(\Omega) = \sum_n \frac{2\sin(n\pi b/L)\sin(n\pi a/L)}{\rho L(1 - r_n^2)p_n^2} \tag{10}$$

where $r_n = \Omega/p_n$, p_n being the natural frequency of the nth mode of a simple beam. Using Eqs. (10) and (8), w_{b1} may be shown to be, for the case $a = b = L/2$,

$$w_{b1} = \frac{2p_0 - 2k(w_{b1} + \tfrac{3}{4}\,\epsilon w_{b1}^3)}{\rho L p_1^2(1 - r_1^2)} \tag{11}$$

Defining the dimensionless parameters

$$\alpha_1^2 = p_1^2/k/m \text{ (spring characteristic)}$$

$$y = kw_{b1}/p_0 \text{ (displacement)}$$

$$\mu = \tfrac{3}{4}\epsilon\,(p_0/k)^2 \text{ (characteristic force)}$$